Frictional behavior of synthetic gouge-bearing faults under the operation of pressure solution

Kyuichi Kanagawa

Department of Earth Sciences, Chiba University, Chiba 263-8522, Japan

Two recent experimental studies on the frictional behavior of synthetic gouge-bearing faults under the operation of pressure solution are compared. One is triaxial shear experiments on quartz gouge at high pressure-temperature hydrothermal conditions (Kanagawa *et al.*, 2000), and the other is rotary shear experiments on halite gouge at atmospheric pressure and room temperature in the presence of methanol-water mixtures (Bos *et al.*, 2000). In spite of quite different experimental settings and conditions, the results of these two series of experiments are strikingly similar; both cataclasis and pressure solution being active during the experiments, gouge strength rate-controlled by cataclasis, two different frictional behaviors of slip hardening and softening, slip hardening associated with gouge compaction, distributed deformation and wall-rock failure, slip softening associated with localized slip along the gouge–wall-rock interface, and the transition from slip-hardening to slip-softening behavior according to decreasing rate of pressure solution. Although there is a difference in velocity dependence of strength between quartz and halite gouges, these similarities clearly demonstrate the important effects of pressure solution on the frictional behavior of gouge-bearing faults.

1. Introduction

Seismogenic faulting in the continental crust mostly occurs at depths of 5–20 km at lithostatic pressures of 100–400 MPa and temperatures of 100–350°C (Sibson, 1983; Scholz, 1990). Under these pressure-temperature conditions and in the presence of water, pressure solution is likely to be an important deformation mechanism (McClay, 1977; Rutter, 1983). The important role of pressure solution in crustal faulting is indicated by widespread occurrence of quartz veins and slickenfibers in exhumed fault zones (e.g. Durney and Ramsay, 1973; Cox *et al.*, 1991; Boullier and Robert, 1992; Cox, 1995; Hickman *et al.*, 1995). The effects of pressure solution on the frictional behavior of faults must therefore be properly evaluated in order to achieve a more realistic understanding of strength and stability of seismogenic faults.

Two different experimental studies have recently investigated the effects of pressure solution on the frictional behavior of synthetic gouge-bearing faults. Kanagawa *et al.* (2000) have conducted triaxial shear experiments on synthetic quartz gouge at a temperature of 927°C and a pressure of 300 MPa in the presence of water, while Bos *et al.* (2000) have conducted rotary shear experiments on synthetic halite gouge at room temperature and atmospheric pressure in the presence of methanol-water mixtures. In these studies, the rate of pressure solution was varied either by gouge grain size or displacement rate (Kanagawa *et al.*, 2000), or by pore fluid composition (Bos *et al.*, 2000). Both studies revealed strikingly similar effects of pressure solution on the frictional behavior of synthetic gouge-bearing faults. In this

paper, I first summarize experimental results on quartz and halite gouges, then discuss their similarities and differences as well as their common implications for the frictional behavior of natural gouge-bearing faults under the operation of pressure solution.

2. Quartz Gouge Experiments

Kanagawa *et al.* (2000) have conducted shear experiments of ≈1 mm thick layer of quartz gouge sandwiched by a pair of sawcut wall-rock cylinders of porous quartz sandstone using a gas-medium triaxial testing apparatus (Paterson, 1990) at a temperature of 927°C, a confining pressure of 300 MPa, a pore water pressure of 200 MPa, and nominally constant axial displacement rates V of 0.13–6.68 μm/s. They used two types of angular, natural quartz powder to simulate fine and coarse gouges. Approximately 98% of each is smaller than 5 μm and 250 μm in diameter, respectively, and their average (by weight) grain sizes are ≈2 μm and ≈45 μm, respectively.

Two different types of frictional behavior, which are dependent on gouge grain size and displacement rate, were observed. Fine gouge at $V \approx 0.6$ μm/s and coarse gouge at $V = 0.13$–0.35 μm/s exhibited continuous slip hardening with increasing displacement, so that coefficients of friction reach to 0.7 (Fig. 1(a)). A gradual stress drop at the end of an experiment (#3946; Fig. 1(a)) was due to failure of the wall-rock sandstone. The slightly higher strength of coarse gouge at $V = 0.35$ μm/s (#3951) than that at $V = 0.13$ μm/s (#3950) (Fig. 1(a)) indicates a positive velocity dependence of strength during slip hardening. Gouges are strongly compacted and very cohesive after experiments. Deformation is distributed across the whole gouge layer (Fig. 2(a)), and in-
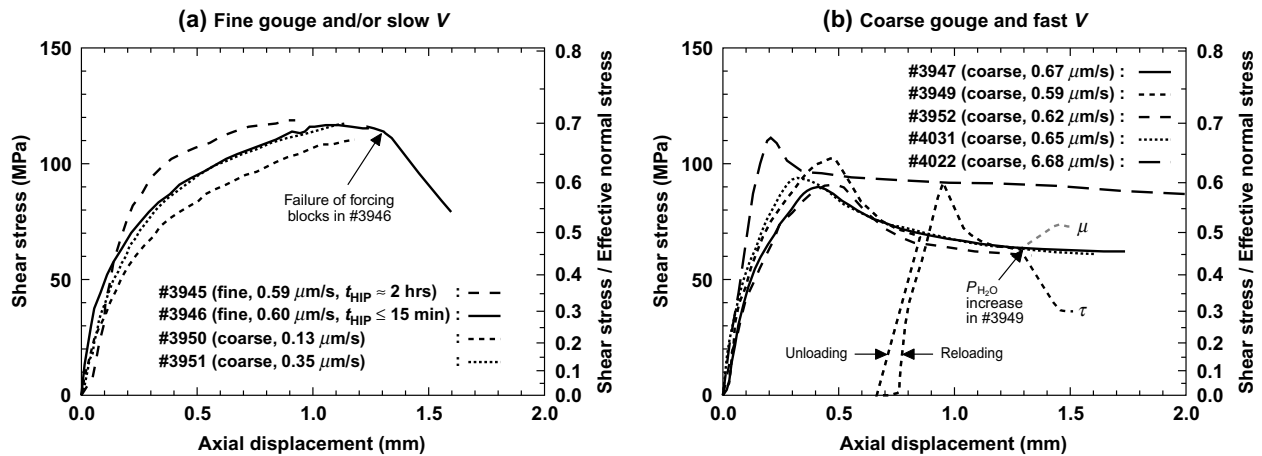
Fig. 1. Slip-hardening (a) and slip-softening (b) behaviors of quartz gouge sheared at 927°C, 300 MPa confining pressure and 200 MPa pore water pressure (Kanagawa *et al.*, 2000). Shear stress along the gouge layer (left-side ordinate) and coefficient of friction (right-side ordinate) are plotted as a function of axial displacement. Fine: fine gouge (≤ 5 μm), coarse: coarse gouge (≤ 250 μm), and t_{HIP}: duration time of hot isostatic pressing before loading. Axial displacement rates are shown in μm/s. After increasing pore pressure in #3949 at a point indicated by an arrow in (b), coefficient of friction is plotted by a gray dashed curve (μ), while shear stress (τ) is plotted as the same as before pore pressure increase.

volves cataclastic processes such as intergranular cracking and slip along R_1 Riedel shears (Fig. 2(a)), as well as compaction accommodated by pressure solution as illustrated by grain interlocking (Fig. 2(b)), grain interpenetration and dissolution pits (Fig. 2(c)).

In contrast, coarse gouge at $V \geq 0.6$ μm/s exhibited a distinct peak stress followed by slip softening and subsequent quasi-stable sliding with coefficients of friction as low as 0.45 (Fig. 1(b)). The shear strength during quasi-stable sliding is higher at $V = 6.68$ μm/s than at $V \approx 0.6$ μm/s (Fig. 1(b)), indicating a positive velocity dependence of strength. The reduced shear strength after an increase in pore water pressure at the end of an experiment (#3949) (Fig. 1(b)) indicates a dependence of strength on effective pressure. Slip softening is associated with slip localization along the upper gouge–wall-rock interface (Fig. 2(d)). Cataclastic deformation and grain size reduction are observed adjacent to the slip surface (Fig. 2(d)). The operation of pressure solution is evident on slip surfaces as well as within the gouge layer as illustrated by euhedral grain growth (Fig. 2(e)), grain interpenetration and dissolution pits (Fig. 2(f)).

3. Halite Gouge Experiments

Bos *et al.* (2000) have conducted shear experiments of ≈ 1 mm thick layer of halite gouge sandwiched by a pair of halite wall-rock rings using a rotary shear apparatus at room temperature, atmospheric pressure, normal stresses of 0.5–3 MPa, and sliding velocities V of 0.01–5 μm/s, in the presence of methanol-water mixtures with water content X of 0–100%. Samples were first sheared at dry conditions to ≈ 5 mm displacement, and subsequently sheared under wet conditions without interrupting experiments. Pore fluid pressure was kept at atmospheric pressure. Stepping of either V or normal stress was also performed at the end of experiments. They used granular halite gouge with initial average grain sizes of normally ≈ 100 μm, and additionally ≈ 50 μm and ≈ 200 μm.

Halite gouge exhibited a distinct peak stress upon adding water-bearing pore fluid, followed by two different types of frictional behavior dependent on pore fluid water content X (Fig. 3(a)). Halite gouge with $X > 35\%$ exhibited quasi-stable sliding accompanied by gradual slip hardening with increasing displacement (Fig. 3(a)). Gouges and gouge–wall-rock interfaces are cohesive after experiments, but the wall rock had failed. Cataclastic deformation is indicated by grain size reduction and slip along R_1 Riedel shears (Fig. 4(a)), while the operation of pressure solution is evident from microstructures such as grain interpenetration and overgrowth (Fig. 4(b)).

In contrast, halite gouge with $X = 10\%$ exhibited pronounced slip softening with regular stick slip (Fig. 3(a)). Slip softening is associated with localized slip along the upper gouge–wall-rock interface (Fig. 4(c)). Grain size reduction is observed adjacent to the slip surface (Fig. 4(c)). The gouge layer itself is a compact aggregate with rounded grains and few cracks. Halite gouge with $X = 35\%$ exhibited transitional behavior, with stable sliding at $V = 1$ μm/s but with stick slip occurring at $V = 5$ μm/s.

A clear linear relationship between shear stress and normal stress was established for all experiments (Fig. 5(a)). The coefficient of friction (line slope in Fig. 5(a)) increases with increasing pore fluid water content X from ≈ 0.25 for $X = 0\%$, through ≈ 0.5 for $X = 10\%$ and ≈ 0.7 for $X = 35\%$, to 0.8–1 for $X = 65$–100% (Fig. 5(a)). Slip-hardened gouge exhibited no clear velocity dependence of strength, while slip-softened gouge exhibited a weak negative velocity dependence (Fig. 5(b)). Halite gouge also showed no systematic grain-size dependence of strength (Fig. 3(b)).

4. Discussion
4.1 Comparison of quartz and halite gouge experiments

The rate of pressure solution was varied in different ways in the above two series of experiments. Kanagawa *et al.* (2000) tested two different gouge grain sizes and displacement rates ranging over one and a half orders of magni-
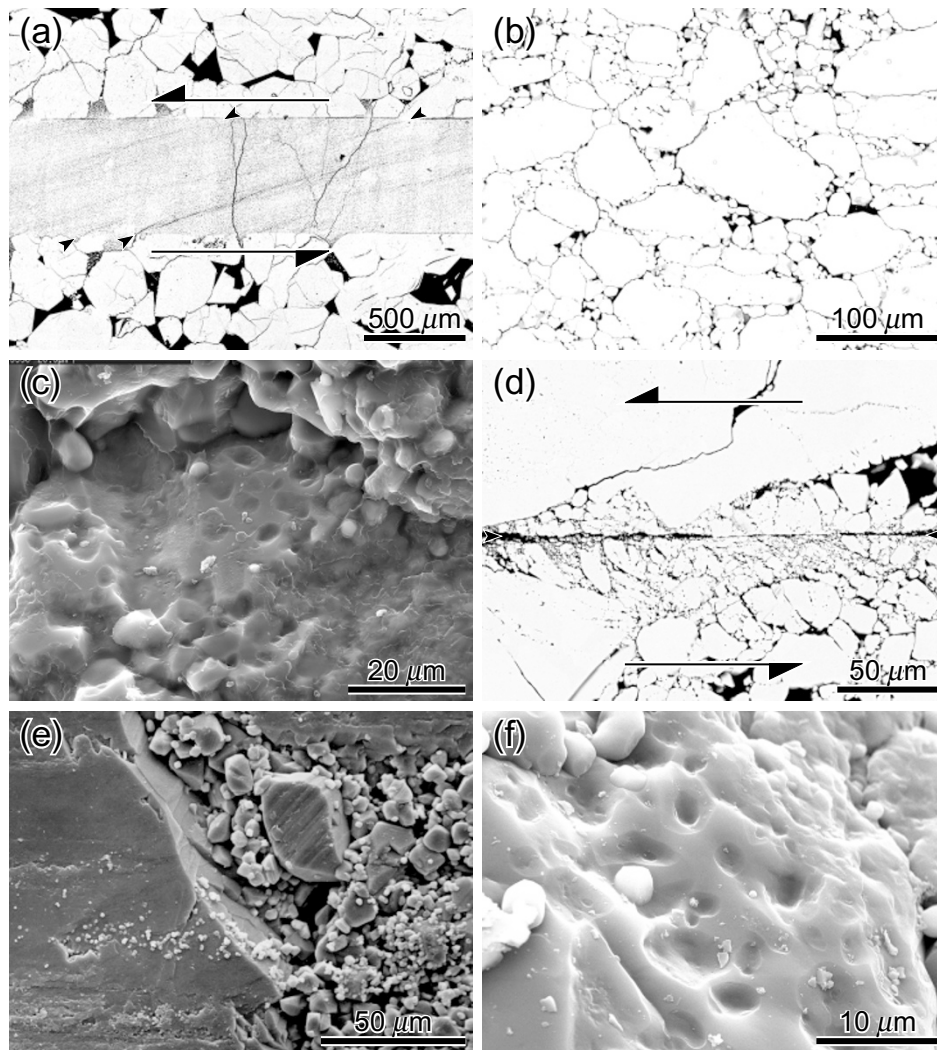
Fig. 2. Microstructures of quartz gouge sheared at 927°C, 300 MPa confining pressure and 200 MPa pore water pressure (Kanagawa *et al.*, 2000). (a), (b) and (d) are back-scattered electron micrographs, while (c), (e) and (f) are secondary electron micrographs. Shear sense is indicated by a pair of arrows in (a) and (d). (a) Slip-hardened fine gouge (#3946) at $V \approx 0.6$ μm/s. R_1 Riedel shears (arrowheads) are developed. (b) Slip-hardened coarse gouge (#3950) at $V \approx 0.13$ μm/s. Gouge grains are significantly interlocking, and their boundaries interpenetrate. (c) Hand-cracked grain surfaces of #3950 showing abundant pits due to grain interpenetration. Flaky appearance is due to the presence of impregnated epoxy on grain surfaces. (d) Slip-softened coarse gouge (#4022) at $V = 6.68$ μm/s. A continuous slip surface (arrowheads) is present along the upper interface between the gouge layer (lower) and wall-rock sandstone (upper). Note cataclastic deformation and grain size reduction adjacent to the slip surface. (e) Slip surface on wall-rock sandstone of slip-softened coarse gouge (#3947) at $V \approx 0.6$ μm/s. Euhedral quartz crystals are present in a pocket on the right of a sandstone grain. (f) Hand-cracked grain surface of slip-softened coarse gouge (#3949) at $V \approx 0.6$ μm/s, on which abundant pits due to grain interpenetration are present. Some small grains are still sitting on the pits.

tude. The rate of pressure solution increases with decreasing gouge grain size or displacement rate at a given temperature (Rutter, 1976; Raj, 1982; Spiers and Schutjens, 1990; Spiers *et al.*, 1990; Dewers and Hajash, 1995). While Bos *et al.* (2000) tested five different water contents in the pore fluid of methanol-water mixtures. The solubility of halite in methanol-water mixtures increases with water contents (Baykara and Pharr, 1991), while the rate of diffusion-controlled pressure solution increases with increasing solubility (Rutter, 1976; Pharr and Ashby, 1983; Gratier and Giguet, 1986). Increasing water contents in the pore fluid is therefore expected to increase the rate of pressure solution.

In spite of quite different experimental settings and conditions, the results of quartz and halite gouge experiments are strikingly similar in many ways. Microstructures of specimens clearly indicate that both cataclasis and pres-

sure solution were active during the two series of experiments. Cataclastic microstructures include R_1 Riedel shears (Figs. 2(a) and 4(a)), continuous slip surfaces (Figs. 2(d) and 4(c)), and grain size reduction along these shears and slip surfaces, while microstructures indicative of pressure solution include grain interpenetration (Figs. 2(b) and 4(b)), dissolution pits (Fig. 2(c) and (f)) and euhedral overgrowth (Figs. 2(e) and 4(b)). The strength of slip-hardened quartz gouge is not so sensitive to gouge grain size and displacement rate as predicted by pressure solution creep (Fig. 1(a); cf. Rutter, 1976; Raj, 1982; Spiers and Schutjens, 1990). The strength of slip-softened quartz gouge is dependent on effective pressure (Fig. 1(b)). The strength of halite gouge is also linearly dependent on normal stress (Fig. 5(a)). Thus deformations of both quartz and halite gouges were still rate-controlled by cataclasis, in spite of clear microstructural ev-
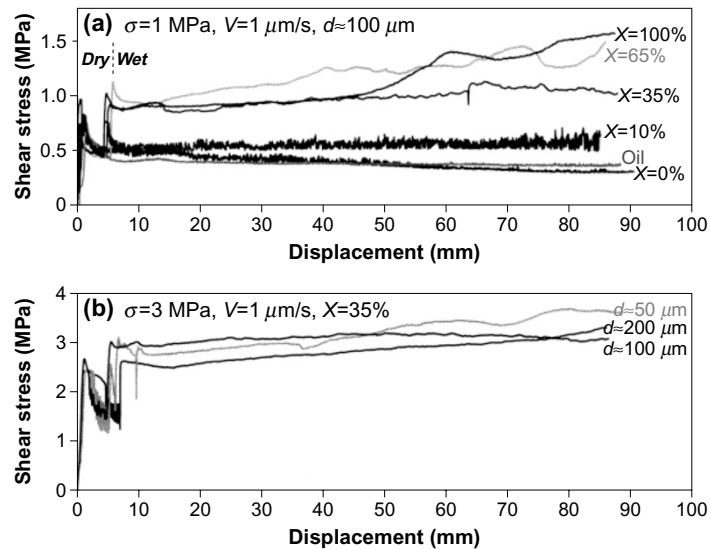
Fig. 3. Mechanical behavior of halite gouge with variable pore fluid water contents X (a) and with different initial grain sizes d (b) sheared at room temperature and atmospheric pressure (Bos *et al.*, 2000). Shear stress is plotted as a function of displacement. Oil in (a) is an experiment using silicone oil as pore fluid. Normal stress is 1 MPa in (a) and 3 MPa in (b). Sliding velocity is 1 μm/s in both (a) and (b). Initial grain size in (a) is $\approx$100 μm, and pore fluid water content in (b) is 35%.
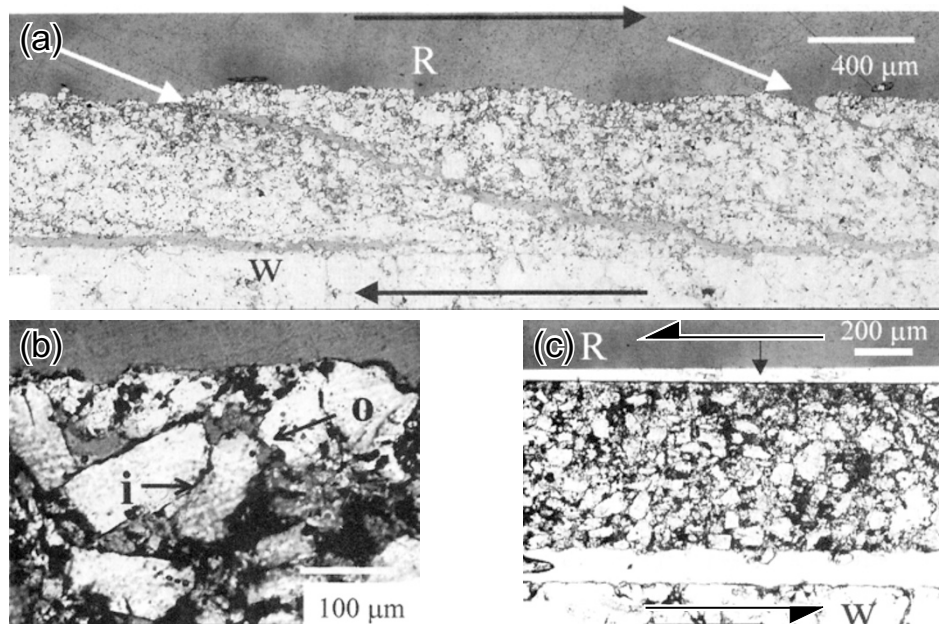

Fig. 4. Optical microstructures of halite gouge sheared at room temperature, atmospheric pressure, 1 MPa normal stress and 1 μm/s sliding velocity (Bos *et al.*, 2000). All micrographs are taken under plane-polarized light. W: wall rock material, and R: epoxy resin. (a) Slip-hardened gouge (N1) with pore fluid water contents $X = 100\%$. R_1 Riedel shears (white arrows) are developed. (b) The same gouge as (a) showing grain interpenetration **i** and overgrowth **o**. (c) Slip-softened gouge (N7) with $X = 10\%$. White material on the top and bottom of the gouge layer is glue. The flat top interface is a localized slip surface in this specimen.

idence for the operation of pressure solution.

Both quartz and halite gouges exhibited two different types of behavior: slip hardening and slip softening. In quartz gouge, slip hardening occurs for fine gouge or at slower displacement rates ($V \leq 0.35$ μm/s), while slip softening occurs for coarse gouge at faster displacement rates ($V \geq 0.6$ μm/s) (Fig. 1). In halite gouge, stable sliding and slip hardening occur for higher pore fluid water contents ($X \geq 35\%$), while slip softening and stick slip occur

for lower pore fluid water contents ($X \leq 35\%$) (Fig. 3(a)). Thus in both quartz and halite gouge experiments, pressure solution is less favored in slip-softened gouges than in slip-hardened gouges. In addition in quartz gouge experiments, cataclasis is more favored for slip-softened coarse gouge than for slip-hardened fine gouge, because fracture strength of grains decreases with increasing grain size (Petch's law; cf. Scholz, 1990). The transition from slip-hardening to slip-softening behavior therefore corresponds to decreasing rate
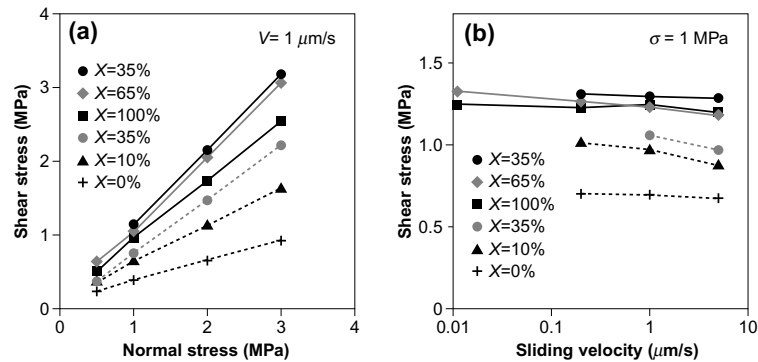
Fig. 5. (a) Shear stress plotted against normal stress (a) and sliding velocity (b) for halite gouge with variable pore fluid water contents X (Bos *et al.*, 2000). Normal-stress stepping at a sliding velocity of 1 μm/s (a), and sliding-velocity stepping at 1 MPa normal stress (b) were performed after displacements of 85–90 mm shown in Fig. 3(a). Dashed lines indicate stick-slip experiments.

of pressure solution and/or increasing cataclastic deformation in both quartz and halite gouges.

Both slip-hardened quartz and halite gouges show distributed deformation throughout the gouge layer, as indicated by compaction and distributed slip along R_1 Riedel shears (Figs. 2(a) and 4(a)). Time-dependent compaction of gouge by pressure solution and resultant progressive increase in load-bearing contact area contribute to slip hardening (Kanagawa *et al.*, 2000; Bos *et al.*, 2000). The failure of wall rock during slip hardening of quartz and halite gouges indicates that the gouge compacted by pressure solution eventually exceeded the failure strength of wall rock in these slip-hardened experiments.

Slip-softening of both quartz and halite gouges is associated with slip localization along the upper gouge–wall-rock interface (Figs. 2(d) and 4(c)). Fluid-assisted healing of the interface was not sufficient to result in its failure in the slip-softened experiments due to the lower rates of pressure solution than in the slip-hardened experiments (Bos *et al.*, 2000). The reduced strength during interface sliding (Figs. 1(b) and 3(a)) is attributed to the much smaller load-bearing area of asperity contacts between the slip surfaces than that of grain-to-grain contacts within the gouge layer before slip softening, as well as to the role of fluid films and dissolution processes in modifying the resistance to frictional sliding (Kanagawa *et al.*, 2000).

Although grain size is a critical factor affecting the mechanical behavior of quartz gouge, it does not apparently affect gouge strength, because no difference in strength during initial slip hardening exists between fine and coarse gouges at $V \approx 0.6$ μm/s (Fig. 1). Halite gouge also shows no systematic grain-size dependence of strength (Fig. 3(b)).

Only a big difference between quartz and halite gouges is velocity dependence of strength. Quartz gouge exhibited a clear positive velocity dependence of strength, i.e. velocity strengthening, during both behaviors of slip hardening and slip softening (Fig. 1). Velocity strengthening is interpreted to be a response to increased cataclastic processes at faster displacement rates, fragmenting gouge grains, and thereby increasing the number of grain-to-grain or asperity contacts and the load-bearing contact area (Kanagawa *et al.*, 2000). Interface sliding after slip softening of quartz gouge was quasi-stable, as predicted by its velocity strengthening. In

contrast, halite gouge exhibited a rather neutral velocity dependence of strength in the slip-hardened experiments, and a weak negative velocity dependence of strength, i.e. velocity weakening, in the slip-softened experiments (Fig. 5(b)). Stick slip occurred during slip softening and subsequent interface sliding of halite gouge, as predicted by its velocity weakening. Stick slip is interpreted to be due to fluid-assisted healing of the gouge–wall-rock interface and its failure (Bos *et al.*, 2000). Although no explanation is given for velocity weakening by Bos *et al.* (2000), it may be due to that increasing sliding velocity leads to decreasing rate of fluid-assisted healing, and thereby interface strength. The reason for the difference in velocity dependence of strength between quartz and halite gouges is unknown at present. Dissolution of fragmented grains produced by cataclastic deformation may be so fast in halite gouge that cataclastic deformation may have not affected the load-bearing grain or asperity contact area as much as in quartz gouge.

4.2 Implications for natural gouge-bearing faults

Although quartz gouge experiments by Kanagawa *et al.* (2000) and halite gouge experiments by Bos *et al.* (2000) are too simplified to apply their results directly to natural gouge-bearing faults, the strikingly similar results of these two series of experiments suggest some common implications for the frictional behavior of gouge-bearing faults under the operation of pressure solution.

The transition from slip-hardening to slip-softening behavior according to decreasing rate of thermally activated pressure solution predicts that this transition also occurs with decreasing temperature (Kanagawa *et al.*, 2000). Along a crustal-scale, gouge-bearing fault under conditions which favor pressure solution, we can thus expect a depth where this transition occurs, which is dependent primarily on temperature, but also on displacement rate and gouge grain size. Above this transitional depth, the fault would exhibit slip softening associated with slip localization along the gouge–wall-rock interface, and subsequent stick slip or quasi-stable interface sliding with low strength. Fluid-assisted healing of the interface and its failure is responsible not only for stick slip (Bos *et al.*, 2000), but may also for recurrence of earthquake faulting (Angevine *et al.*, 1982). Slip softening itself may also represent a new variety of instability which can control rupture nucleation and recurrence independently

on velocity dependence of strength (Kanagawa *et al.*, 2000). Because slip during slip softening is much slower than that during stick slip (Fig. 3), the former may represent slow earthquakes. Below the transitional depth, the fault would exhibit stable sliding with high strength accompanied by slip hardening and distributed deformation, and become as strong as or even stronger than its wall rocks, while its strength is still rate-controlled by cataclasis. Earthquake faulting below this depth may not be nucleated along the fault, but by failure of wall rocks.

References

Angevine, C. L., D. L. Turcotte, and M. D. Furnish, Pressure solution lithification as a mechanism for the stick slip behavior of faults, *Tectonics*, **1**, 151–160, 1982.

Baykara, T. and G. M. Pharr, Effects of liquid phases on intrinsic interfacial sliding of alkali halide crystals, *Acta Metall. Mater.*, **39**, 1141–1150, 1991.

Bos, B., C. J. Peach, and C. J. Spiers, Slip behavior of simulated gouge-bearing faults under conditions favoring pressure solution, *J. Geophys. Res.*, **105**, 16,699–16,717, 2000.

Boullier, A.-M. and F. Robert, Paleoseismic events recorded in Archaean gold-quartz vein networks, Val d'Or, Abitibi, Quebec, Canada, *J. Struct. Geol.*, **14**, 161–179, 1992.

Cox, S. F., Faulting processes at high fluid pressures: An example of fault valve behaviour from the Wattle Gully Fault, Victoria, Australia, *J. Geophys. Res.*, **100**, 12,841–12,859, 1995.

Cox, S. F., V. J. Wall, M. A. Etheridge, and T. F. Potter, Deformational and metamorphic processes in the formation of mesothermal vein-hosted gold deposits—examples from the Lachlan Fold Belt in central Victoria, Australia, *Ore Geol. Rev.*, **6**, 391–423, 1991.

Dewers, T. and A. Hajash, Rate laws for water-assisted compaction and stress-induced water-rock interaction in sandstones, *J. Geophys. Res.*, **100**, 13,093–13,112, 1995.

Durney, D. W. and J. G. Ramsay, Incremental strains measured by syntectonic crystal growths, in *Gravity and Tectonics*, edited by K. A. De Jong and R. Scholten, pp. 67–96, John Wiley, New York, 1973.

Gratier, J. P. and R. Giguet, Experimental pressure solution-deposition on quartz grains: The crucial effect of the nature of the fluid, *J. Struct. Geol.*, **8**, 845–856, 1986.

Hickman, S., R. Sibson, and R. Bruhn, Introduction to special section: Mechanical involvement of fluids in faulting, *J. Geophys. Res.*, **100**, 12,831–12,840, 1995.

Kanagawa, K., S. F. Cox, and S. Zhang, Effects of dissolution-precipitation processes on the strength and mechanical behavior of quartz gouge at high-temperature hydrothermal conditions, *J. Geophys. Res.*, **105**, 11,115–11,126, 2000.

McClay, K. R., Pressure solution and Coble creep in rocks and minerals: A review, *J. Geol. Soc. London*, **134**, 57–70, 1977.

Paterson, M. S., Rock deformation experimentation, in *The Brittle-Ductile Transition in Rocks, Geophys. Monogr. Ser., 56*, edited by A. G. Duba *et al.*, pp. 187–194, AGU, Washington, D.C., 1990.

Pharr, G. M. and M. F. Ashby, On creep enhanced by a liquid phase, *Acta Metall.*, **31**, 129–138, 1983.

Raj, R., Creep in polycrystalline aggregates by matter transport through a liquid phase, *J. Geophys. Res.*, **87**, 4731–4739, 1982.

Rutter, E. H., The kinetics of rock deformation by pressure solution, *Phil. Trans. R. Soc. London, Ser. A*, **283**, 203–219, 1976.

Rutter, E. H., Pressure solution in nature, theory and experiment, *J. Geol. Soc. London*, **140**, 725–740, 1983.

Scholz, C. H., *The Mechanics of Earthquakes and Faulting*, 439 pp., Cambridge Univ. Press, New York, 1990.

Sibson, R. H., Continental fault structure and the shallow earthquake source, *J. Geol. Soc. London*, **140**, 741–767, 1983.

Spiers, C. J. and P. M. T. M. Schutjens, Densification of crystalline aggregates by fluid-phase diffusional creep, in *Deformation Processes in Minerals, Ceramics and Rocks*, edited by D. J. Barber and P. G. Meredith, pp. 334–353, Unwin Hyman, London, 1990.

Spiers, C. J., P. M. T. M. Schutjens, R. H. Brezesowsky, C. J. Peach, J. L. Liezenberg, and H. J. Zwart, Experimental determination of constitutive parameters governing creep of rocksalt by pressure solution, in *Deformation Mechanisms, Rheology and Tectonics*, edited by R. J. Knipe and E. H. Rutter, Geol. Soc. Spec. Publ., **54**, 215–227, 1990.

K. Kanagawa (e-mail: kyu@earth.s.chiba-u.ac.jp)